A mutation in the ribosomal protein uS12 reveals novel functions of its universally conserved PNSA loop

Madhurima Datta[1], Maalavika Pillai[1], Mamata Jayant Modak[1], Aivar Liiv[2], Faisal Tarique Khaja[3], Tanweer Hussain[3], Jaanus Remme[2] and Umesh Varshney[1,4,*]

[1]***Department of Microbiology and Cell Biology***, Indian Institute of Science, Bangalore, 560012, India.

[2]***Institute of Molecular and Cell Biology***, University of Tartu, Riia 23, 51010 Tartu, Estonia.

[3]***Department of Molecular Reproduction, Development and Genetics,*** Indian Institute of Science, Bangalore, 560012, India.

[4]***Jawaharlal Nehru Centre for Advanced Scientific Research***, Bangalore, 560064, India.

***Correspondence to Umesh Varshney:** Department of Microbiology and Cell Biology, Indian Institute of Science, Bangalore, 560012, India. Phone: +91 80 22932686, Fax: +91 80 23602697, Email: *varshney@iisc.ac.in*

Fig. S1

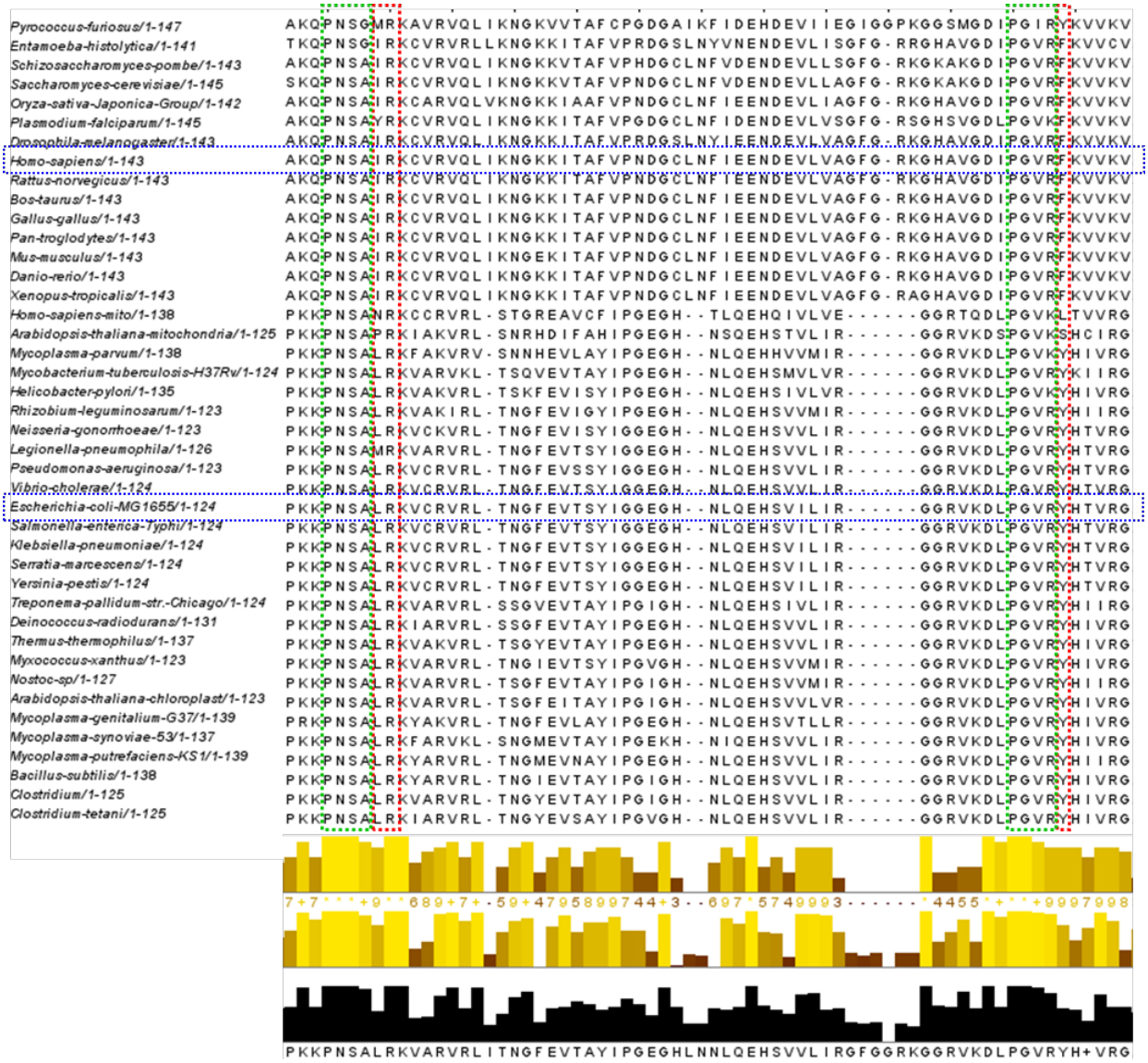

Fig. S1: Multiple sequence alignment of uS12 sequences. The sequence of uS12 protein or its eukaryotic ortholog (RPS23) from 42 different organisms (including organelles) spanning all three kingdoms of life were procured and aligned. Among them, the sequences for the human and *E. coli* proteins are demarcated in blue. The conserved loop sequences PNSA and PGVR are shown in green box. Residues L48, R49 and Y94 (*E. coli* numbering), which have been subjects of this study, are demarcated in red.

Fig. S2A

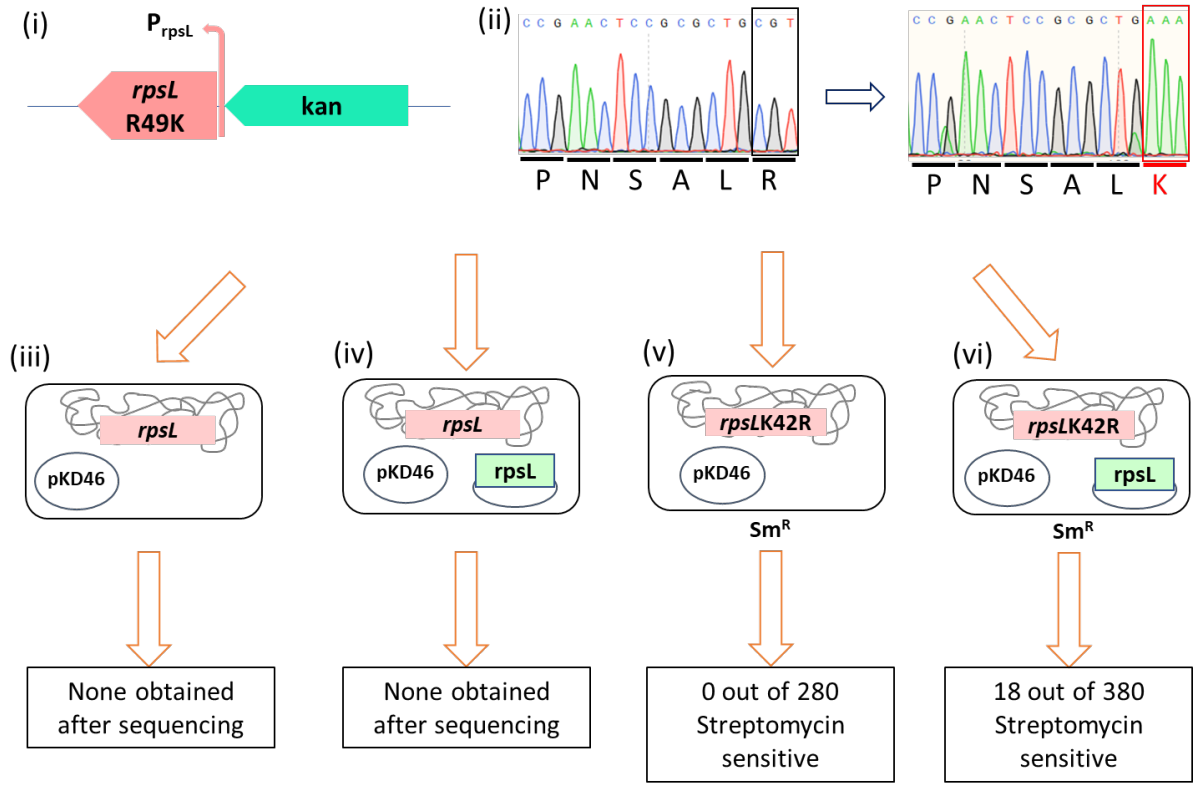

Fig. S2A: Generation of KL16 *rpsL*R49K mutant. (i) Schematic representation of the linear DNA amplicon for electroporation. **(ii)** Chromatogram representing sequence of the mutated locus from R49 to K49. **(iii)** Electroporation of *rpsL*R49K:*kan* linear fragment into KL16 pKD46. Slower growing transformants were expected. However, upon sequencing the Kan^R transformants from slightly slower growing colonies several times, we found that they did not carry the mutation. This meant that the recombination had occurred between the kanamycin cassette and in a region 5' to the R49K mutation in the *rpsL* gene body or that colony size cannot be used for selection. **(iv)** Electroporation of *rpsL*R49K:*kan* into KL16/pKD46 supported by pACDH*rpsL*. To increase our chances of getting the mutation, we tried the knock-in in the presence of pACDH*rpsL*. However, this too failed, as difference in colony size could no longer be used as a screen. **(v)** Electroporation of *rpsL*R49K:*kan* into KL16 Sm^R/pKD46. The strain LJ14 has a variation in S12, which renders it naturally resistant to streptomycin. The allele responsible for this was K42R, which is situated just seven amino acids away from our interest R49. We transduced this streptomycin resistance-conferring allele from LJ14 to KL16 via bacteriophage P1 mediated transduction, then tried the recombination in this background. The linear DNA fragment contains streptomycin sensitive allele. Therefore, we screened the transformants obtained for loss of streptomycin resistance, exploiting that high chances exist for them to be R49K mutants because of the close linkage between the two alleles. After having screened many colonies, this approach too failed. **(vi)** Electroporation of *rpsL*R49K:*kan* into KL16 Sm^R/pKD46 supported by pACDH*rpsL*. We thought of using the above approach in conjunction with pACDH*rpsL* support, again, in case the R49K mutation alone is toxic to cells. Finally, we got 18 colonies, which were streptomycin sensitive.

Fig. S2B

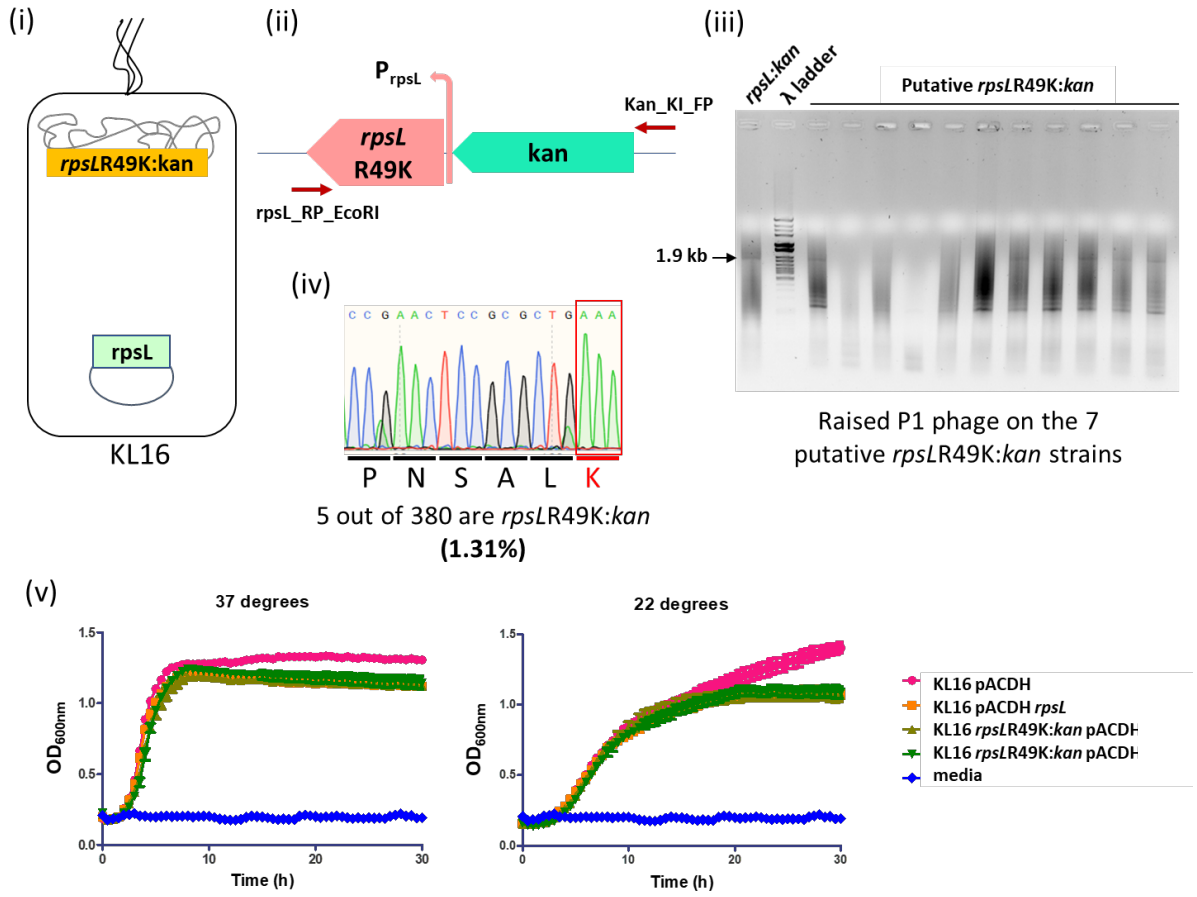

Fig. S2B: Verification of *rpsL*R49K mutant. **(i)** Diagram depicting the strain generated (in Figure S2A (vi)). **(ii)** Diagram representing primer locations. **(iii)** PCR to verify *rpsL*R49K:*kan* mutation in the putative mutants. From the 18 colonies that were Sm^S, we performed colony PCR to confirm that the kanamycin resistance was genuinely due to the cassette we have knocked-in. Seven out of 18 putative R49K mutants gave us the desired 1.9 kb band as is seen in the positive control (lane 1). Immediately, we raised P1 bacteriophage lysates on the 7 strains and transduced KL16 Sm^R strain to transfer the R49K mutation to avoid recombination of the genomic mutant copy with the plasmid-borne wild type. **(iv)** Chromatogram showing results of sequencing. We sequenced the uS12 coding gene from all the 7 strains and found 5 of them to contain the genomic mutation. (v) Growth curve with the parent and the mutants generated (upward and downward green triangles) at 37 °C and 22 °C. We performed a growth curve with the parent and the mutant strains and observed that there is no difference in growth perhaps because the multicopy plasmid-borne wild type gene suffices for healthy growth of the cells if they wish to avoid incorporation of the mutant S12 into the ribosomes. The fact that we don't get this mutant alone without wild type support is indicative of R49K being a lethal mutation in bacteria which possess a haploid genome.

Fig. S2C.

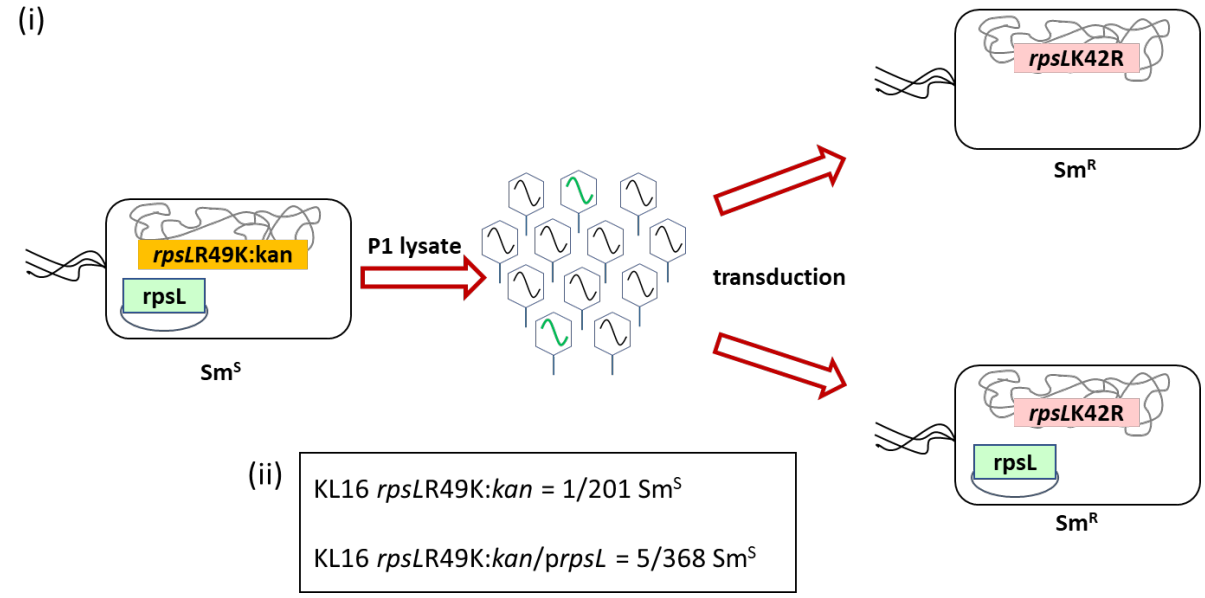

Fig. S2C: Final attempt at generation of the *rpsL*R49K mutant. (i) Pictorial representation of raising bacteriophage P1 lysate on *rpsL*R49K:*kan*/pACDH*rpsL* and transduction into Sm^R KL16 strains with and without wild type *rpsL* support on plasmid. (ii) Results after screening the transductants for Sm^S phenotype. Upon sequencing the *rpsL* locus, only the 5 with pACDH*rpsL* support were found to contain the R49K mutation.

Fig. S3

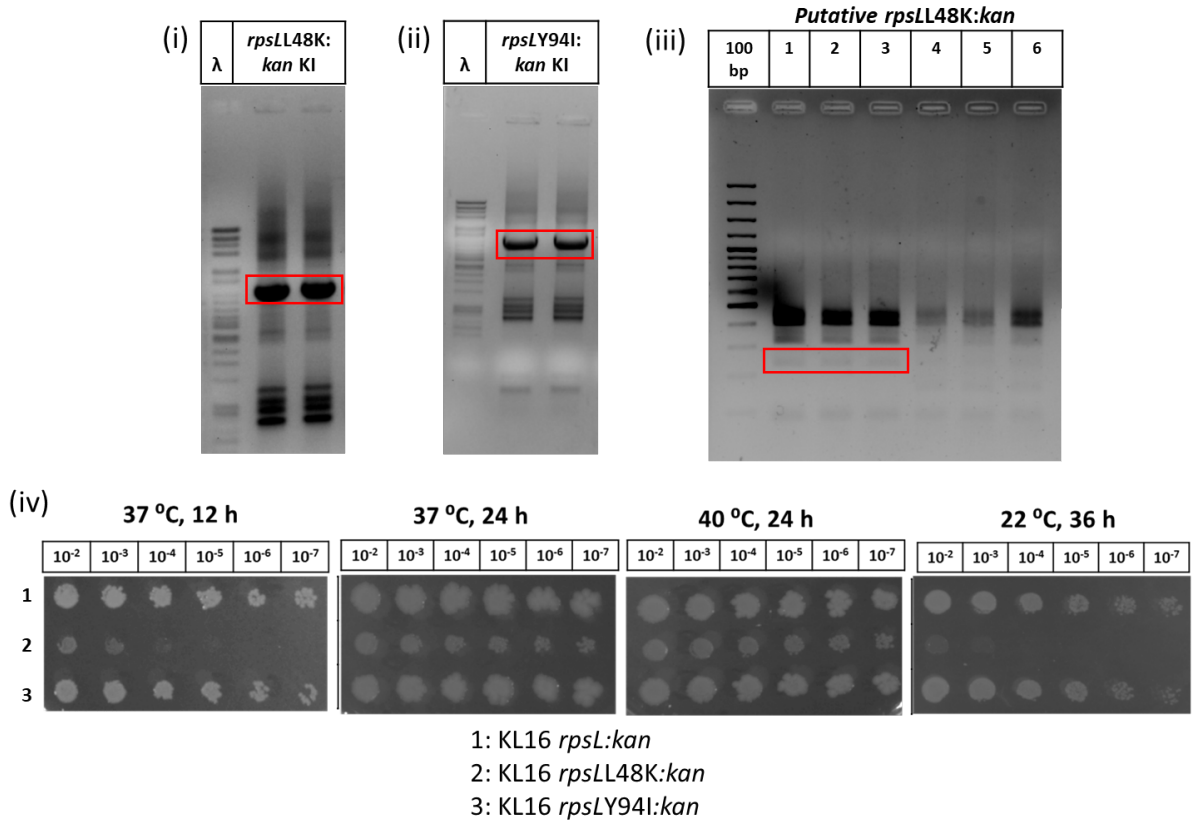

Fig. S3: Generation of *rpsL*L48K and *rpsL*Y94I mutants. (i) *rpsL*L48K:*kan* (both lanes) and (ii) *rpsL*Y94I:*kan* (both lanes) were amplified from plasmid (1741 bp) for electroporation into KL16/pKD46. (iii) Screening of KL16 *rpsL*L48K:*kan* transformants by RFLP. The mutation giving rise to L48K causes a loss of a HhaI restriction site in the gene amplicon. Lanes 1-3, smaller colonies which contain the L48K mutation and lanes 4-6, larger colonies which do not contain the L48K mutation according to banding pattern predicted in Fig. 2C (iv) The L48K allele is detrimental to *E coli*. The L48K allele grows much slower compared to wild type and is cold sensitive. The Y94I allele shows no defect in growth (N=3, n=3).

Fig. S4

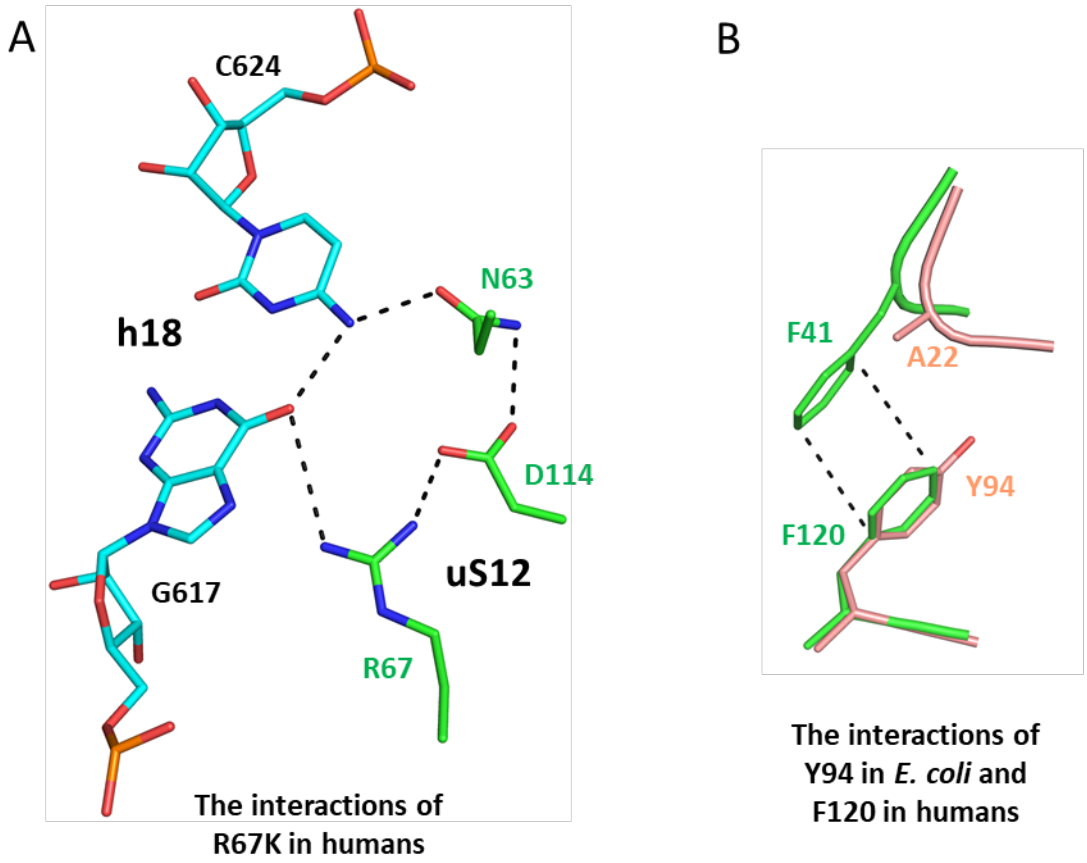

Fig. S4: A. The network of interactions identified around R67 of RPS23 in humans (black dotted lines) from existing structural data. **B.** The amino acid equivalents Y94 in *E. coli* and F120 in humans in an overlapping image depicting pi-pi interaction of F120 with the nearby F41 (in humans). The corresponding amino acid to F41 is alanine in *E. coli*, negating the possibility of such an intramolecular interaction.

Fig. S5

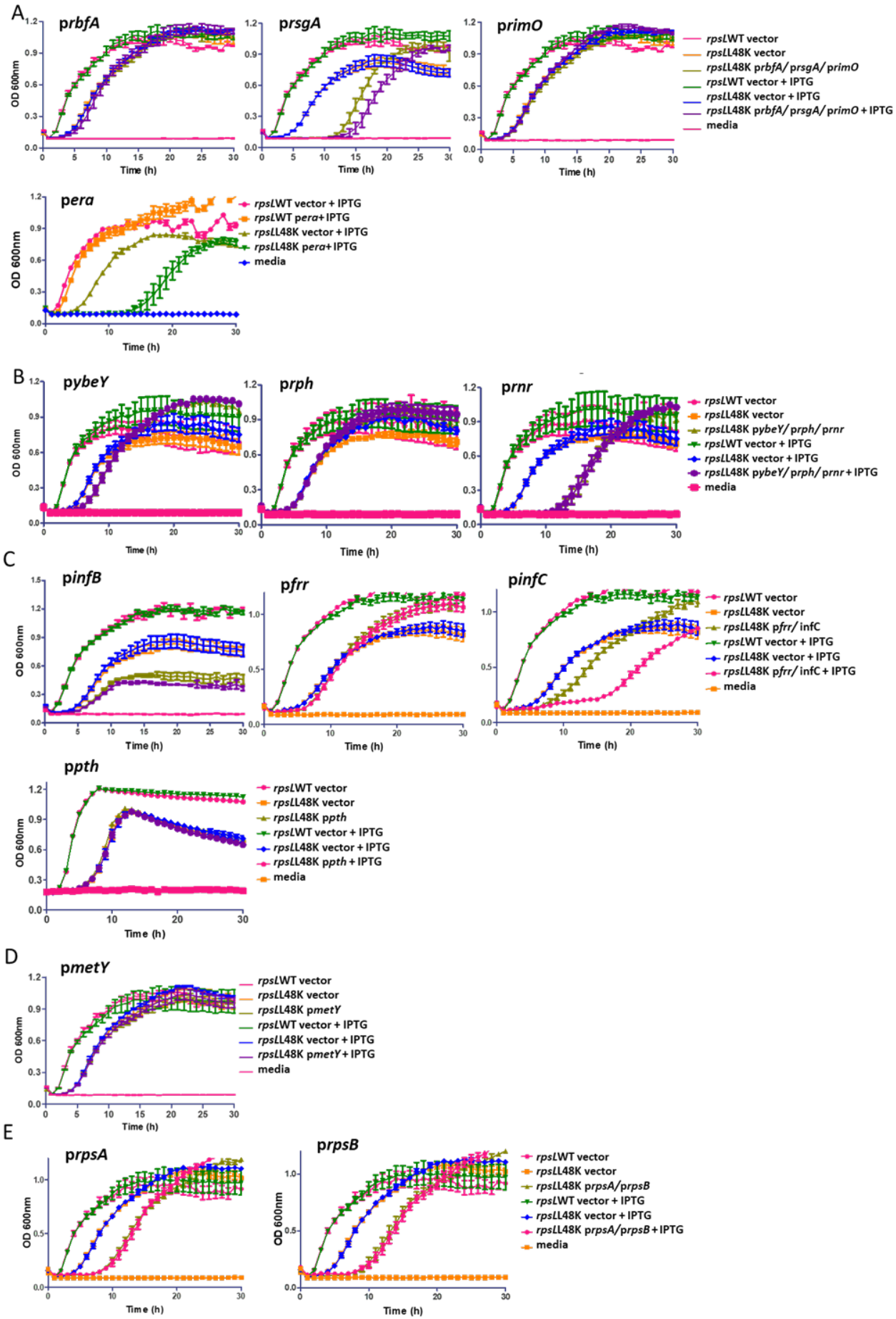
A
prbfA
prsgA
primO
OD 600nm
Time (h)
rpsLWT vector
rpsLL48K vector
rpsLL48K prbfA/ prsgA/ primO
rpsLWT vector + IPTG
rpsLL48K vector + IPTG
rpsLL48K prbfA/ prsgA/ primO + IPTG
media
pera
rpsLWT vector + IPTG
rpsLWT pera+ IPTG
rpsLL48K vector + IPTG
rpsLL48K pera+ IPTG
media
B
pybeY
prph
prnr
rpsLWT vector
rpsLL48K vector
rpsLL48K pybeY/ prph/ prnr
rpsLWT vector + IPTG
rpsLL48K vector + IPTG
rpsLL48K pybeY/ prph/ prnr + IPTG
media
C
pinfB
pfrr
pinfC
rpsLWT vector
rpsLL48K vector
rpsLL48K pfrr/ infC
rpsLWT vector + IPTG
rpsLL48K vector + IPTG
rpsLL48K pfrr/ infC + IPTG
media
ppth
rpsLWT vector
rpsLL48K vector
rpsLL48K ppth
rpsLWT vector + IPTG
rpsLL48K vector + IPTG
rpsLL48K ppth + IPTG
media
D
pmetY
rpsLWT vector
rpsLL48K vector
rpsLL48K pmetY
rpsLWT vector + IPTG
rpsLL48K vector + IPTG
rpsLL48K pmetY + IPTG
media
E
prpsA
prpsB
rpsLWT vector
rpsLL48K vector
rpsLL48K prpsA/prpsB
rpsLWT vector + IPTG
rpsLL48K vector + IPTG
rpsLL48K prpsA/prpsB + IPTG
media

Fig. S5: Overexpression to alleviate the growth defect in *rpsL*L48K. The growth defect due to *rpsL*L48K cannot be rescued by over expression of **A.** 30S subunit biogenesis factors like RbfA, RsgA, RimO, or Era; **B.** 16S rRNA 3'-end processing enzymes like YbeY, RNaseR, or RNasePH; **C.** factors that participate in translation like IF2, IF3, RRF, or Pth; **D.** initiator tRNA; E. Ribosomal proteins bS1, uS2. (N=3, n=4). We hypothesized that by over-expressing ribosome biogenesis factors for the SSU, we may assist ribosome biogenesis trapped in unfavorable states, towards a more favorable conformation. None could rescue the growth defect. Noticeably, over-expression of RsgA GTPase conferred a further disadvantage (Fig. S4A, p*rsgA*). Similar observations were obtained with Era GTPase (Fig. S4A, p*era*). Both function towards the tail end of SSU assembly (Razi et al., 2019). It is disputed if RsgA and uS12 can compete for SSU binding, given their overlapping binding pockets and time of entry into the scheme of SSU biogenesis (Jomaa et al., 2011). The presence of the mutant uS12 may affect the recruitment of RsgA and hence, its function in driving towards a more stable SSU structure. If the SSU structure is somewhat distorted, it can affect processing further downstream. Further, when we over-expressed RNases involved in 16S rRNA 3' end maturation, there was no improvement. Over-expression of RNaseR, a multifunctional RNAse (Fig. S4B, p*rnr*) provided growth disadvantage. This may be attributed to the other roles of RNaseR in the cell (Chen and Deutscher, 2005; Domingues et al., 2015; Hossain et al., 2016). Over-expression of initiation factors is known to be detrimental to cells and so was the case with IF2 and IF3 overexpression (Fig. S4C, p*infB* and p*infC*). Over-expression of ribosome recycling factor (RRF) and the i-tRNA (Rao and Varshney, 2002; Shetty and Varshney, 2016) from *frr* and *metY* genes, respectively, too could not rescue the growth (Fig. S4C and Fig. S4D). Over-expression of the last two proteins recruited in SSU assembly, bS1 and uS2 too hampered the growth (Fig. S4E).

Fig. S6

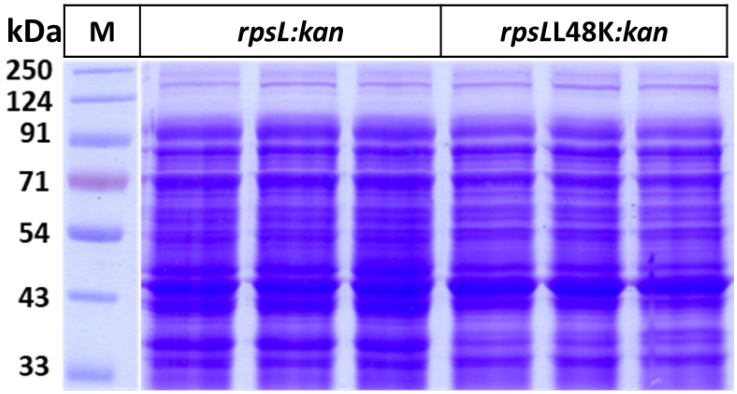

Fig. S6.: Impact of reduced fidelity on the mutant cells. A. Total cellular proteome resolved on a 12% SDS-PAGE and stained by Coomassie blue.

Fig. S7

A

Time (s)	KL16 *rpsL* (OD_{420}/OD_{600})			KL16 *rpsL*L48K (OD_{420}/OD_{600})		
5	0	0	0	0	0	0
30	0.0188	-0.014	0.0658	0.0096	0.0597	0.044
60	0.1001	0.0326	-0.008	0.0194	0.1166	0.0491
90	0.2552	0.0688	-0.035	0.0559	0.1878	0.0486
120	0.157	0.1192	0.0083	0.0283	0.2047	0.0507
150	0.284	0.1516	0.0459	0.3132	0.4862	0.755
180	0.5369	0.1926	0.1758	0.795	0.7425	1.0348
210	0.7901	0.3101	0.4732	1.5417	1.3035	1.3143
240	1.095	0.5125	0.6002	2.2882	2.0419	1.831
270	1.4185	0.5922	0.9028	3.1431	2.5967	2.212

B

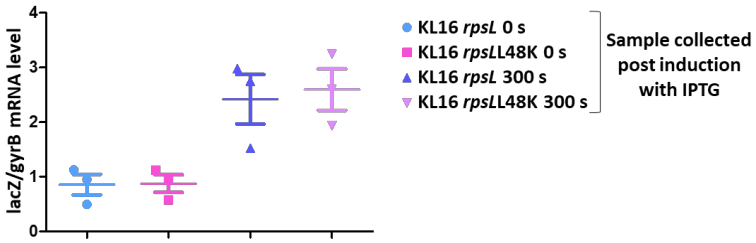

Fig. S7: Raw data for LacZ assay for initiation and elongation rates of translation in wild type vs mutant cells. A. Raw data table with baseline correction used to plot the graph in Fig 4(A). The reading collected at 5 s for each sample was subtracted from all the other values for baseline correction. **B.** mRNA levels of lacZ post induction compared to *gyrB* mRNA (encoding the DNA gyrase subunit B) to check for level of induction post IPTG administration in the wild type and mutant cells. At the said time points, 2 ml of culture was aliquoted and total RNA isolation was carried out by using the Tri Reagent (Sigma). RNA (1 µg) from each was used to convert to cDNA, using the RNA-dependent DNA polymerase, RevertAid enzyme (Thermo Scientific) following the manufacturer's protocol. 50-times diluted cDNA was utilized to perform a semi-quantitative PCR reaction using primers specific to *lacZ* and *gyrB*. The ratio of the two mRNAs at the two time points tested, reveals that the mRNA levels remain comparable. Fig 4(B).

Fig. S8

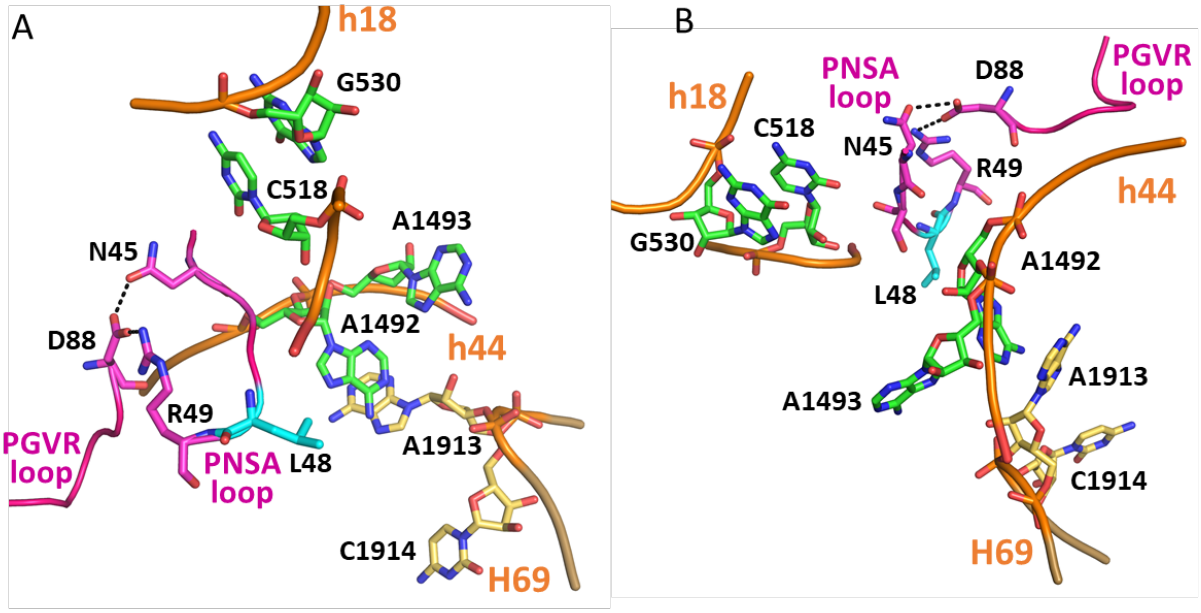

Fig. S8: Interactions between uS12 and rRNA in its vicinity at the A-site of the ribosome. Display of interactions between *E. coli* uS12 (PDB ID: 4V7S, chain AL; PNSA and PGVR loops are colored magenta, Leu48 is depicted in cyan) and 16S rRNA (h44 and h18 depicted in brown backbones), 23S rRNA (H69 depicted in pale yellow backbone). A and B are two different orientations of the same. The PNSA and PGVR loops of uS12 are bridged by polar contacts between Asn45-Asp88-Arg49. A change from the neutral Leu48 to the positively charged Lys48 may affect the above-mentioned contacts. A1492 and A1493 of h44 and G530 of h18 (16S rRNA) interact with and proofread the correctness of the incoming aminoacyl-tRNA against the cognate codon at the A site. If the L48K mutation can perturb the structure at the decoding centre, A1493 may be prone towards stacking with A1913 of the H69 of 23S rRNA, thereby, retracting from its function in proofreading codon anticodon interactions. Overall, a structural change may occur due to the L48K mutation that can account for the various phenotypes studied.

Table S1: Raw data for the loss of fidelity of translation in the *rpsL*L48K mutant.

A

Construct	KL16 *rpsL:kan*		KL16 *rpsL*L48K:*kan*		Fold difference between the relative values (%mutant/%WT)
	LacZ activity (Miller units)	Relative value (% WT)	LacZ activity (Miller units)	Relative value (% mutant)	
pSG25	24868.12 ± 3107.584	100.00	45717.43 ± 4393.224	100.00	1
pSG7	1505.461 ± 159.948	06.05	10153.03 ± 2602.457	22.20	3.707409 ± 0.916
pSG12	1201.725 ± 117.074	04.83	8340.698 ± 1173.866	18.24	3.749 ± 0.213

B

Construct	CAT activity (pmol / µg protein)	
	KL16 *rpsL:kan*	KL16 *rpsL*L48K:*kan*
$pCAT_{am27}$	1.657 ± 0.10	13.575 ± 1.577

C

Construct	KL16 *rpsL:kan*		KL16 *rpsL*L48K:*kan*		Fold difference between the relative values (%mutant/%WT)
	CAT activity (pmol / µg protein)	Relative value (% WT)	CAT activity (pmol / µg protein)	Relative value (% mutant)	
pCAT AUG	243570.1 ± 12549.32	100.00	520165.5 ± 83067.46	100.00	1
pCAT GUG	119638.5 ± 19014.31	49.11	520078.8 ± 60824.24	99.00	2.066 ± 0.09
pCAT UUG	165829.3 ± 10811.66	68.08	511286.7 ± 118581.8	151.10	2.1 ± 0.9
pCAT AUU	6598.75 ± 904.22	2.71	60649.45 ± 2138.727	13.49	5.017 ± 0.1
pCAT AUA	10450.36 ± 696.05	4.29	142240.4 ± 8595.518	30.06	7.002 ± 0.05

D

Construct	KL16 *rpsL:kan*		KL16 *rpsL*L48K:*kan*		Fold difference between the relative values (%mutant/%WT)
	CAT activity (pmol / µg protein)	Relative value (% WT)	CAT activity (pmol / µg protein)	Relative value (% mutant)	
$pCAT_{am1}metY_{CUA}$	18973.38 ± 3880.22	100.00	90606.77 ± 2406.36	100.00	1
$pCAT_{am1}metY_{CUA/3GC}$	1160.576 ± 137.90	6.11	35517.62 ± 3713.23	39.1	6.553 ± 0.73

Table S1: Loss of fidelity of translation in the *rpsL*L48K mutant. The values of biological replicates used in each assay have been tabulated. Panels **A, B, C**, and **D** are raw data tables for Figs. 3A, 3B, 3C and 3E, respectively. For panels C and D, the CAT activity (pmol)/ µg total protein was normalized with beta-lactamase activity (See Experimental procedures, Section 4.6) to account for plasmid copy number of the ampicillin-resistant reporter plasmids. The mean values independently for the strains wild type or L48K for *rpsL* harboring the control plasmid were taken as 100%, and the relative values for the test plasmids were calculated as shown. Fold differences between the relative values of the two strains for the same construct were calculated by taking a ratio of the relative values of the strains harboring the L48K/WT alleles of *rpsL*. For A and C, N=3, n=3; for B and D, N=3, n=4.

Table S2: Prediction of the changes in interactions between uS12 and transiently interacting proteins in light of the L48K or equivalent mutation in different organisms by *in silico* analysis

Organism	PDB ID	Resolution of solved structure (Å)	Interaction identified	Remarks
H. sapiens	3JAH, 3JAI	3.45	uS12 I66K: steric clash with eS30 G4	The presence of a cognate codon-anticodon pair at the ribosomal A-site stabilizes the N-terminus of eS30 that allows His76 (eS30) to contact the anticodon, A1824 and A1825. The contacts formed, thus, are important in decoding at the A-site. A steric clash between uS12 I66K and eS30 N terminus may not sufficiently order the N-terminus of eS30 to subsequently relay the necessary signals.
K. lactis	6FYY	3.02	uS12 I68K: steric clash with eIF1A D90	The C-terminal and N-terminal tails of eIF1A plays an important role in mRNA scanning and start codon recognition. uS12 contacts the oligonucleotide binding domain of eIF1A. uS12 I68K may weaken binding of eIF1A to the 40S ribosome.
E. coli	6GXM	3.80	uS12 L48K: interacts with RF1 S304 (d = 3.2 Å) and D305 (d = 2.7 Å)	Prolonged interaction of the ribosome with a release factor may delay ribosome recycling after UAG, UAA stop codons.
E. coli	5H5U	3.01	uS12 L48K: steric clash with RF2 W319	The switch loop of RF2, which connects domains 3 and 4 of RF2 undergo a significant structural rearrangement upon encountering a stop codon. A steric clash between W319 of the switch loop of RF2 and uS12 L48K may affect lodging of the GGQ motif at the stop codon site resulting in difficulty in termination at UGA and UAA stop codons
E. coli	3JA1	3.60	uS12 L48K: interacts with EFG E558 (d = 4.7 Å)	This additional ionic interaction may cause slower release of EF-G, delaying/compromising its capability in fidelity of elongation.
E. coli	6O7K	4.20	uS12 L48K: interacts with IF1 R64 (d = 2.9 Å) and G65 (d = 2.5 Å)	A stronger interaction between IF1 and uS12 L48K may cause a delayed departure of the IF1 from the 70S, prolonging final steps of ribosome maturation and translation initiation.
E. coli	5IQR	3.00	uS12 L48K: interacts with $tRNA^{Phe}$ A26 (d = 3.7 Å)	uS12 L48K in E coli and L52K in *T. thermophilus* may establish novel contacts with the A-site tRNA.
T. thermophilus	4V5P	3.10	uS12 L52K: interacts with $tRNA^{Trp}$ A26 (d = 4.9 Å)	
T. thermophilus	4V5L	3.10	uS12 L52K: interacts with $tRNA^{Trp}$ C27 (d = 4.0 Å)	
T. thermophilus	4V8Q	3.10	uS12 L52K: steric clash with SmpB D40	uS12 L52K may hinder binding of SmpB, resulting in slower release of stalled polypeptide-mRNA complexes.
T. thermophilus	4V5E	3.45	uS12 L52K: interacts with RF2 G308 (d = 3.34 Å)	uS12 L52K may prolong residence of RF2 resulting in delay in termination at UGA and UAA stop codons.
T. Thermophilus	4V9H	2.86	uS12 L52K: interacts with EFG E548 (d = 4.3 Å)	This additional ionic interaction may cause slower release of EF-G, delaying/compromising its capability in fidelity of elongation (also noted in *E. coli*).
T. thermophilus	1HR0	3.2	uS12 L52K: interacts with IF1 E56 (d = 2.9 Å), T58 (d = 4.0 Å), R64 (d = 3.4 Å)	A stronger interaction between IF1 and uS12 L48K may cause a delayed departure of the IF1 from the 70S, prolonging final steps of ribosome maturation and translation initiation (also noted in *E. coli).*

Table S3: List of strains used in this study

***E. coli* strains**	**Genotype**	**Reference**
KL16	K-12, *thi1*, *relA*1, *spoT*1	(Low, 1968)
TG1	*supE hsd5*$^{-}$ *thi*$^{-}$ (*lac-proAB*) F' [*traD*36 *proAB*$^{+}$ *lacI*^{q} *lacZ*ΔM15]	(*Sambrook*, 1989)
BW25113	(*araD-araB*)*567 lacZ4787*(::*rrnB-3*) λ- *rph-1* (*rhaDrhaB*)*568 hsdR514*)	(Baba et al., 2006)
LJ14	*E. coli* MC1061 harboring a temperature sensitive allele *frr*^{ts} (*frr14*)	(Janosi, 1998)
AA7852	CP78 (F-, *arg* -, *leu* -, *thr* -, *his* -, *thiamine* -, *relA* +, T1^{s}) harbouring a temperature-sensitive *pth* allele (*pth*^{ts})	(Atherly and Menninger, 1972)
KL16 *rpsL:kan*	KL16 with *rpsL* gene tagged with kan^{R} cassette upstream	This study
KL16 *rpsL*L48K*:kan*	KL16 *rpsL:kan* with codon for Leucine48 of uS12 mutated to Lysine (CTG to AAA)	This study
KL16 *rpsL*R49K*:kan*	KL16 *rpsL:kan* with codon for Arginine49 of uS12 mutated to Lysine (CGT to AAA)	This study
KL16 *rpsL*Y94*:kan*	KL16 *rpsL:kan* with codon for Tyrosine94 of uS12 mutated to Isoleucine (TAC to ATT)	This study
BW25113 *rpsL:kan*	*E. coli* BW25113 with *rpsL* gene tagged with kan^{R} cassette upstream	This study
BW25113 *rpsL*L48K*:kan*	BW25113 *rpsL:kan* with codon for Leucine48 of uS12 mutated to Lysine (CTG to AAA) by bacteriophage P1 mediated transduction	This study
LJ14 *rpsL:kan*	LJ14 with *rpsL* gene tagged with kan^{R} cassette upstream	This study
LJ14 *rpsL*L48K*:kan*	LJ14 *rpsL:kan* with codon for Leucine48 of uS12 mutated to Lysine (CTG to AAA) by bacteriophage P1 mediated transduction	This study
AA7852 *rpsL:kan*	AA7852 strain with *rpsL* gene tagged with kan^{R} cassette upstream	This study
AA7852 *rpsL*L48K*:kan*	AA7852 *rpsL:kan* with codon for Leucine48 of uS12 mutated to Lysine (CTG to AAA) by bacteriophage P1 mediated transduction	This study

Table S4: List of plasmids used in this study

Plasmids	Details	Reference
pACDH	Plasmid with ACYC ori of replication, which is compatible with plasmids possessing ColE1 ori of replication; contains lac promoter and Tet^R	(Rao and Varshney, 2002)
pKD46	Plasmid harboring λ Red recombination genes (γ, β and *exo*) and a *ts* ori of replication, Amp^R	(Datsenko and Wanner, 2000)
pACDH *rpsL* (p*rpsL)*	uS12 cloned in pACDH vector at NcoI EcoRI sites.	This study
pACDH *rpsL*L48K	pACDH *rpsL* with mutation from Leu to Lys at 48th codon	This study
pACDH *rpsL*R49K	pACDH *rpsL* with mutation from Arg to Lys at 49th codon	This study
pACDH *rpsL*Y94I	pACDH *rpsL* with mutation from Tyr to Ile at 94th codon	This study
pSG25	Plasmid containing wild-type *lacZ*	(O'Connor, 1997)
pSG7	LacZ is produced from this plasmid only by a +1 frameshift at the 7th amino acid during translation	(O'Connor, 1997)
pSG12	LacZ is produced from this plasmid only by a -1 frameshift at the 12th amino acid during translation	(O'Connor, 1997)
$pCAT_{AUG}$	Renamed from pRSVCAT2.5	(Varshney and RajBhandary, 1990)
$pCAT_{GUG}$	Initiation codon of $pCAT_{AUG}$ mutated to GUG	(Arora et al., 2013)
$pCAT_{UUG}$	Initiation codon of $pCAT_{AUG}$ mutated to UUG	(Arora et al., 2013)
$pCAT_{AUU}$	Initiation codon of $pCAT_{AUG}$ mutated to AUU	(Arora et al., 2013)
$pCAT_{AUA}$	Initiation codon of $pCAT_{AUG}$ mutated to AUA	(Arora et al., 2013)
$pCAT_{amber1}$ $metY_{CUA}$	pBR322 derivative plasmid harbouring the CAT reporter gene where UAG serves as the initiation codon (renamed from pRSVCATam1.2.5) and containing i-tRNA gene *metY* with a cognate CUA anticodon	(Das et al., 2008)
$pCAT_{amber1}$ $metY_{CUA/3GC}$	$pCAT_{amber1}$ $metY_{CUA}$ plasmid with the additional mutation in the 3GC base pairs in the anticodon stem of i-tRNA gene to that of sequence in elongator met tRNA	(Mandal et al., 1996)
$pCAT_{amber27}$	pCAT plasmid with UAG codon at the 27th amino acid position	(Kapoor et al., 2011)
pTrc *rbfA* (p*rbfA*)	RbfA cloned in pTrc99C vector at NcoI EcoRI sites.	This study
pTrc *rimO* (p*rimO*)	RimO cloned in pTrc99C vector at NcoI EcoRI sites.	This study
pACDH *era* (p*era*)	Era cloned in pACDH vector	K. Lahry (unpublished)
pACDH *rsgA* (p*rsgA*)	RsgA cloned in pACDH vector	S. Singh (unpublished)
pACDH *ybeY* (p*ybeY*)	YbeY cloned in pACDH vector	(Shetty and Varshney, 2016)
pACDH *rph* (p*rph*)	RNasePH cloned in pACDH vector	
pACDH *rnr* (p*rnr*)	RNaseR cloned in pACDH vector	
pACDH *infB* (p*infB*)	IF2 cloned in pACDH vector	(Gaur et al., 2008)
pACDH *infC* (p*infC*)	IF3 cloned in pACDH vector	(Singh et al., 2008)
pACDH *frr* (p*frr*)	RRF cloned in pACDH vector	(Singh, 2004)
pACDH *Bsub pth*	Pth from *Bacillus subtilis* cloned in pACDH vector	(Singh, 2004)
pRSV *metY* (p*metY)*	i-tRNA cloned in pRSV vector, Amp^R	(Samhita et al., 2012)
pNT3 *rpsA* (p*rpsA)*	bS1 cloned in pNT3 vector, Amp^R	(Saka, 2005)
pNT3 *rpsB* (p*rpsB)*	uS2 cloned in pNT3 vector, Amp^R	(Saka, 2005)

Table S5: List of oligonucleotides used in this study

DNA oligomer	Sequence	Reference
rpsL_kan_KI_FP	AGCACCCCAGCCAGATGGCCTGGTGATGGCGG GATCGGGCCTTTCGTTTTATG	This study
rpsL_kan_KI_RP	GCCGAATTTTAGGGCGATGCCGAAAAGGTGTC AAGATGTTGTAGGTGGAC	This study
rpsL_RP_NcoI	GTTGCCATGGAATAGCTCCTGG	This study
rpsL_FP_NcoI	CCAGGAGCTATTCCATGG	This study
rpsL_FP_EcoRI	CCGGAATTCCGTTAAGCCTTAG	This study
rpsL_up_FP	ATATTTCTTGACACCTTTTCG	This study
rpsL_dn_RP	TTAGTTTGACATTTAAGTTAAAA	This study
rpsL_L48K_FP	CGAACTCCGCGAAACGTAAAGTATG	This study
rpsL_L48K_RP	CATACTTTACGTTTCGCGGAGTTCG	This study
rpsL_R49K_FP	AACTCCGCGCTGAAAAAAGTATGCCGTG	This study
rpsL_R49K_RP	CACGGCATACTTTTTTCAGCGCGGAGTT	This study
rpsL_Y94I_FP	CGGGTGTTCGTATTCACACCGTACG	This study
rpsL_Y94I_RP	CGTACGGTGTGAATACGAACACCCG	This study
rbfA_FP_NcoI	TTTACCATGGCGAAAGAATTTG	This study
rbfA_RP_EcoRI	AGGAGAATTCATTAGTCCTCCTTG	This study
rimO_FP_NcoI	TAAGCCATGGGCAAAG TAACTC	This study
rimO_RP_EcoRI	GCCTGAATTCATTAAACCCGGC	This study
lacZ_fp1	CTAATCACGACGCGCTGTATC	This study
lacZ_rp1	GCCTGCCAGTATTTAGCGAAAC	This study
gyrB_fp	GCGGTTGAACAGCAGATGAAC	This study
gyrB_rp	CCAGGTACAGTTCGGAAAGC	This study
16S	TCTTCGCGTTGCATCGAATT	(Shetty and Varshney, 2016)
17S	TGTGTGAGCACTGCAAAGAACGCTTTAAGG	(Shetty and Varshney, 2016)
23S	CGCGCAGGCCGACTCGACCAGTGAGC	(Shetty and Varshney, 2016)
Met33	CTTCGGGTTATGAGCCCGACGAGCTA	(Shetty et al., 2014)

References

Arora, S., Bhamidimarri, S.P., Bhattacharyya, M., Govindan, A., Weber, M.H.W., Vishveshwara, S., Varshney, U., 2013. Distinctive contributions of the ribosomal P-site elements m2G966, m5C967 and the C-terminal tail of the S9 protein in the fidelity of initiation of translation in Escherichia coli. Nucleic Acids Res. 41, 4963–4975. https://doi.org/10.1093/nar/gkt175

Atherly, A.G., Menninger, J.R., 1972. Mutant E. coli Strain with Temperature Sensitive Peptidyltransfer RNA Hydrolase. Nature. New Biol. 240, 245–246. https://doi.org/10.1038/newbio240245a0

Baba, T., Ara, T., Hasegawa, M., Takai, Y., Okumura, Y., Baba, M., Datsenko, K.A., Tomita, M., Wanner, B.L., Mori, H., 2006. Construction of *Escherichia coli* K-12 in-frame, single-gene knockout mutants: the Keio collection. Mol. Syst. Biol. 2. https://doi.org/10.1038/msb4100050

Chen, C., Deutscher, M.P., 2005. Elevation of RNase R in Response to Multiple Stress Conditions. J. Biol. Chem. 280, 34393–34396. https://doi.org/10.1074/jbc.C500333200

Das, G., Thotala, D.K., Kapoor, S., Karunanithi, S., Thakur, S.S., Singh, N.S., Varshney, U., 2008. Role of 16S ribosomal RNA methylations in translation initiation in Escherichia coli. EMBO J. 27, 840–851. https://doi.org/10.1038/emboj.2008.20

Datsenko, K.A., Wanner, B.L., 2000. One-step inactivation of chromosomal genes in Escherichia coli K-12 using PCR products. Proc. Natl. Acad. Sci. 97, 6640–6645. https://doi.org/10.1073/pnas.120163297

Domingues, S., Moreira, R.N., Andrade, J.M., dos Santos, R.F., Bárria, C., Viegas, S.C., Arraiano, C.M., 2015. The role of RNase R in trans-translation and ribosomal quality control. Biochimie 114, 113–118. https://doi.org/10.1016/j.biochi.2014.12.012

Gaur, R., Grasso, D., Datta, P.P., Krishna, P.D.V., Das, G., Spencer, A., Agrawal, R.K., Spremulli, L., Varshney, U., 2008. A Single Mammalian Mitochondrial Translation Initiation Factor Functionally Replaces Two Bacterial Factors. Mol. Cell 29, 180–190. https://doi.org/10.1016/j.molcel.2007.11.021

Hossain, S.T., Malhotra, A., Deutscher, M.P., 2016. How RNase R Degrades Structured RNA: ROLE OF THE HELICASE ACTIVITY AND THE S1 DOMAIN. J. Biol. Chem. 291, 7877–7887. https://doi.org/10.1074/jbc.M116.717991

Janosi, L., 1998. Evidence for invivo ribosome recycling, the fourth step in protein biosynthesis. EMBO J. 17, 1141–1151. https://doi.org/10.1093/emboj/17.4.1141

Jomaa, A., Stewart, G., Mears, J.A., Kireeva, I., Brown, E.D., Ortega, J., 2011. Cryo-electron microscopy structure of the 30S subunit in complex with the YjeQ biogenesis factor. RNA 17, 2026–2038. https://doi.org/10.1261/rna.2922311

Kapoor, S., Das, G., Varshney, U., 2011. Crucial contribution of the multiple copies of the initiator tRNA genes in the fidelity of tRNA fMet selection on the ribosomal P-site in Escherichia coli. Nucleic Acids Res. 39, 202–212. https://doi.org/10.1093/nar/gkq760

Low, B., 1968. Formation of merodiploids in matings with a class of Rec- recipient strains of Escherichia coli K12. Proc. Natl. Acad. Sci. 60, 160–167. https://doi.org/10.1073/pnas.60.1.160

Mandal, N., Mangroo, D., Dalluge, J.J., McCloskey, J.A., Rajbhandary, U.L., 1996. Role of the three consecutive G:C base pairs conserved in the anticodon stem of initiator tRNAs in initiation of protein synthesis in Escherichia coli. RNA N. Y. N 2, 473–482.

O'Connor, M., 1997. Decoding fidelity at the ribosomal A and P sites: influence of mutations in three different regions of the decoding domain in 16S rRNA. Nucleic Acids Res. 25, 1185–1193. https://doi.org/10.1093/nar/25.6.1185

Rao, A.R., Varshney, U., 2002. Characterization of Mycobacterium tuberculosis ribosome recycling factor (RRF) and a mutant lacking six amino acids from the C-terminal end reveals that the C-terminal residues are important for its occupancy on the ribosome. Microbiology 148, 3913–3920. https://doi.org/10.1099/00221287-148-12-3913

Razi, A., Davis, J.H., Hao, Y., Jahagirdar, D., Thurlow, B., Basu, K., Jain, N., Gomez-Blanco, J., Britton, R.A., Vargas, J., Guarné, A., Woodson, S.A., Williamson, J.R., Ortega, J., 2019. Role of Era in assembly and homeostasis of the ribosomal small subunit. Nucleic Acids Res. 47, 8301–8317. https://doi.org/10.1093/nar/gkz571

Saka, K., 2005. A Complete Set of Escherichia coli Open Reading Frames in Mobile Plasmids Facilitating Genetic Studies. DNA Res. 12, 63–68. https://doi.org/10.1093/dnares/12.1.63

Sambrook J. Molecular Cloning: A Laboratory Manual. NY: Cold Spring Harbor., 1989.

Samhita, L., Shetty, S., Varshney, U., 2012. Unconventional initiator tRNAs sustain Escherichia coli. Proc. Natl. Acad. Sci. 109, 13058–13063. https://doi.org/10.1073/pnas.1207868109

Shetty, S., Nadimpalli, H., Shah, R.A., Arora, S., Das, G., Varshney, U., 2014. An extended Shine–Dalgarno sequence in mRNA functionally bypasses a vital defect in initiator tRNA. Proc. Natl. Acad. Sci. 111, E4224–E4233. https://doi.org/10.1073/pnas.1411637111

Shetty, S., Varshney, U., 2016. An evolutionarily conserved element in initiator tRNAs prompts ultimate steps in ribosome maturation. Proc. Natl. Acad. Sci. 113, E6126–E6134. https://doi.org/10.1073/pnas.1609550113

Singh, N.S., 2004. A physiological connection between tmRNA and peptidyl-tRNA hydrolase functions in Escherichia coli. Nucleic Acids Res. 32, 6028–6037. https://doi.org/10.1093/nar/gkh924

Singh, N.S., Ahmad, R., Sangeetha, R., Varshney, U., 2008. Recycling of Ribosomal Complexes Stalled at the Step of Elongation in Escherichia coli. J. Mol. Biol. 380, 451–464. https://doi.org/10.1016/j.jmb.2008.05.033

Varshney, U., RajBhandary, U.L., 1990. Initiation of protein synthesis from a termination codon. Proc. Natl. Acad. Sci. 87, 1586–1590. https://doi.org/10.1073/pnas.87.4.1586